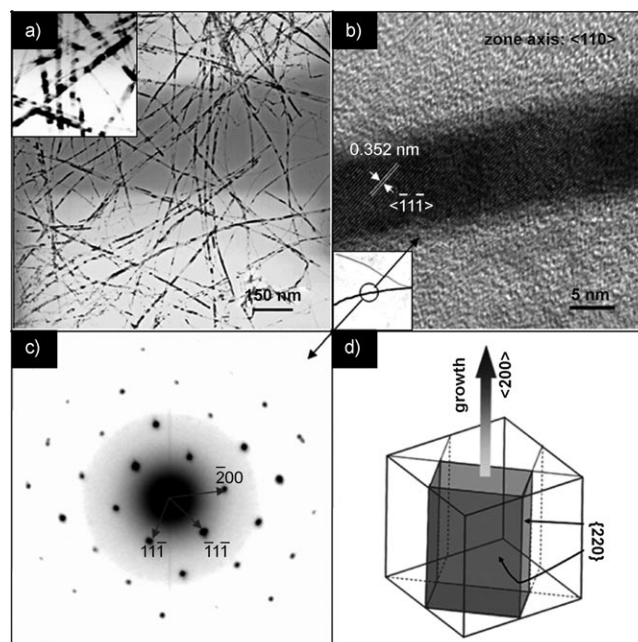


# p-Type Field-Effect Transistors of Single-Crystal Zinc Telluride Nanobelts\*\*

Jun Zhang, Po-Chiang Chen, Guozhen Shen, Jibao He, Amar Kumbhar, Chongwu Zhou, and Jiye Fang\*

Zinc telluride (ZnTe) is a very attractive semiconductor with a direct bandgap of 2.26 eV<sup>[1]</sup> and a Bohr exciton radius of 6.2 nm.<sup>[2]</sup> Although one-dimensional (1D) ZnTe has been prepared by using a pulsed electrochemical deposition method in aqueous solution<sup>[2]</sup> and recently an oriented attachment mechanism in organic solution,<sup>[3]</sup> the reported diameters are much larger than the Bohr exciton radius and its properties have never been explored. Herein, we report a novel strategy, which functions by controlling the direction of crystal growth, for the preparation of ZnTe nanobelts that have electronic transport properties.

The ZnTe synthesis was carried out under a stream of argon at 250 °C using oleylamine as a high-boiling-point solvent in a three-neck flask equipped with a condenser. A transmission electron microscopy (TEM) image of the resulting ZnTe reveals the morphology and nanostructure of the as-prepared straight nanobelts with a typical width of approximately 12 nm and a smooth surface (no discrete particles were observed on the surface; Figure 1 a). The width of the ZnTe nanobelts can be further increased by using longer periods of growth time (up to 30 min; see Figure S1 in the Supporting Information). The ripple-like contrast shown in the inset of Figure 1 a arises from the strain resulting from



**Figure 1.** a) TEM image of ZnTe nanobelts; b) HRTEM image of a selected ZnTe nanobelt (the image projection direction is  $\langle 110 \rangle$ ); c) SAED pattern of ZnTe nanobelts; d) schematic illustration of the growth direction of the ZnTe nanobelts.

the bending of the belt when its thickness is reduced to an extremely small value. This phenomenon has previously been observed in nanobelts of semiconducting oxides and is normal for beltlike nanostructures.<sup>[4]</sup> It also illustrates that the nanobelt is straight along the growth direction. The length range of the nanobelts is from submicrometer to several micrometers. To further investigate the crystal structure, a high-resolution TEM (HRTEM) observation on a single ZnTe nanobelt was also conducted. The HRTEM image and its corresponding selected area electron diffraction (SAED) pattern are shown in Figure 1b and Figure 1c, respectively. The pointed lattice fringes in Figure 1b exhibit a lattice-spacing distance of 0.352 nm, which matches the interplanar spacing of the adjacent  $\{11\bar{1}\}$  lattice planes.<sup>[5]</sup> The SAED pattern confirms this attribution and reveals that the single-crystal nanobelt of cubic ZnTe anisotropically grows along the  $\langle 200 \rangle$  direction (Figure 1d).

To further verify the beltlike morphology, the ZnTe sample was also investigated using both field-emission scanning electron microscopy (FE-SEM) and powder X-ray diffractometry (XRD). The FE-SEM image presented in Figure 2 a shows a beltlike shape. The image of a selected flat

[\*] J. Zhang, Prof. J. Fang  
Department of Chemistry  
State University of New York at Binghamton  
Binghamton, New York 13902 (USA)  
Fax: (+1) 607-777-4478  
E-mail: jfang@binghamton.edu  
Homepage: <http://chem.binghamton.edu/FANG>

P. Chen, Dr. G. Shen, Prof. C. Zhou  
Ming Hsieh Department of Electrical Engineering  
University of Southern California  
Los Angeles, California 90089 (USA)

Dr. J. He  
Coordinated Instrumentation Facility, Tulane University  
New Orleans, Louisiana 70118 (USA)

A. Kumbhar<sup>[†]</sup>  
Electron Microscope Facility, Clemson University  
Anderson, South Carolina 29625 (USA)

[†] present address:  
CHANL Instrumentation Facility  
Institute for Advanced Materials, NanoScience and Technology  
University of North Carolina at Chapel Hill  
Chapel Hill, NC 27599-3216 (USA)

[\*\*] This work was supported by the US NSF (DMR-0731382, CCF-0726815, and CCF-0702204) and by the State University of New York at Binghamton.

Supporting information for this article is available on the WWW under <http://dx.doi.org/10.1002/anie.200804073>.

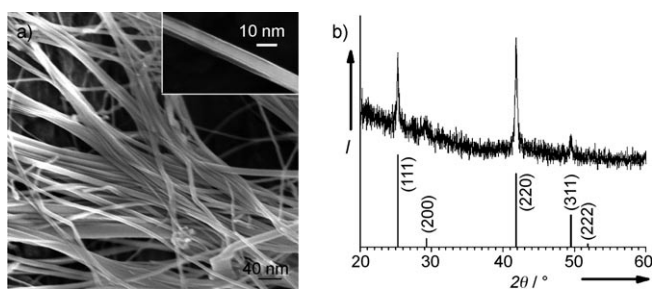


**Figure 2.** a) FE-SEM image of the ZnTe nanobelts. The inset shows a flat belt with an approximate width of 12 nm and a thickness of less than 6 nm. b) XRD patterns of ZnTe nanobelts deposited on a Si wafer.

belt clearly shows an approximate width of 12 nm and thickness of less than 6 nm (see inset of Figure 2a and Figure S2 in the Supporting Information). In the XRD pattern shown in Figure 2b, all of the detected peaks are indexed using a standard diffraction card.<sup>[5]</sup> The relative intensities of the diffraction peaks, which indicate the single phase of zinc blende (sphalerite) structure (space group  $F\bar{4}3m(216)$ ) are shown and labeled in the lower part of Figure 2b. It must be emphasized that the relative intensity of the 220 diffraction peak in Figure 2 is much stronger than that of the 111 peak, with an approximate ratio of 150:100; in contrast, the ratio in the standard card is 80:100.<sup>[5]</sup> This indicates a high probability that the 1D ZnTe is flat, as only a flat “wire” can align its (220) facet upwards<sup>[6]</sup> when it is slowly deposited on a polished substrate (Figure 1d). In fact, the 111 diffraction peak would disappear if all the ZnTe nanobelts were to lay horizontally on the silicon wafer, that is, if they were all strictly “straight”. This observation is the third piece of evidence that supports the formation of nanobelts. As further evidence for the nanobelt morphology, the UV/Vis spectrum of a 1D ZnTe suspension in hexane was recorded. In comparison with the position of the 548 nm (2.26 eV) absorption band edge of bulk ZnTe,<sup>[11]</sup> the suspension has an absorption peak at approximately 350 nm (Figure 3), which reveals not only a high thickness monodispersity but also an apparent blue shift. This finding indicates the occurrence of

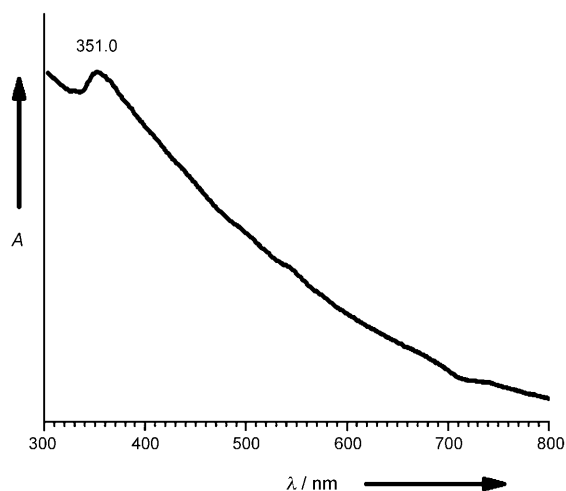


**Figure 3.** UV/Vis spectrum of the ZnTe nanobelts.

the quantum confinement effect, which results from the extremely tight thickness restriction (<6 nm) of the ZnTe nanobelts.

For small crystals formed primarily with the face-centered cubic (fcc) structure, the shape of growth is determined by the minimization of surface energy that is associated with different crystallographic facets, and generally increases in the order of  $\gamma\{111\} < \gamma\{100\} < \gamma\{110\}$ .<sup>[7,8]</sup> This means that an fcc crystal should normally grow by first enlarging the area of {111} facets to minimize the total surface energy. However, this order could be altered by the adsorption of capping molecules as these nanocrystals develop further. Our previous study<sup>[9]</sup> indicates that ZnTe synthesized in benzyl ether with small amounts of oleylamine might grow thermodynamically into nanotetrahedrons at high temperature (250 °C) and grow kinetically into nanorods along the  $\langle 11\bar{1} \rangle$  direction only at low temperature (150 °C). Yong et al.<sup>[3]</sup> prepared 1D ZnTe using oleylamine as solvent at 250 °C, and determined that the growth direction of ZnTe wires is parallel to the [111] direction when large amounts of myristic acid and hexadecylamine were used instead of oleylamine. Comparing these results with our current observations, we conclude that, at high temperature (250 °C) a large amount of oleylamine favors the formation of 1D ZnTe grown along the [100] direction (Figure 1d), whereas the use of a large amount of hexadecylamine with myristic acid under similar conditions leads to the formation of ZnTe wires along the [111] direction. The latter could be prepared in oleylamine only when both the amount of amine and growth temperature were reduced, which indicates that different binding abilities of capping agents on various nanocrystal faces are the key factors that control the behavior of anisotropic growth. The 1D growth of FePt in which the wire-growth direction is parallel to the [100] direction of FePt has been shown to be induced by the self-organization of oleylamine into an elongated reverse micelle-like structure.<sup>[10]</sup> A similar mechanism may also exist in the present ZnTe system.

To explore their electronic transport properties, a suspension of ZnTe nanobelts in hexane was deposited onto a degenerately doped Si wafer, and a selected nanobelt was modified at both ends with electrodes. As shown in Figure 4a, the SEM image indicates that the single nanobelt lies across the gap of approximately 2  $\mu\text{m}$  between the source and the drain electrodes. Figure 4b shows typical current versus source–drain voltage ( $I_{\text{ds}}-V_{\text{ds}}$ ) curves at different gate voltages ( $V_{\text{g}}$ ), obtained from the single ZnTe nanobelt. The  $I_{\text{ds}}-V_{\text{g}}$  curve measured at  $V_{\text{ds}} = 5$  V is shown in Figure 4c. For a given  $V_{\text{ds}}$ ,  $I_{\text{ds}}$  increases with increasing negative  $V_{\text{g}}$ , which clearly implies that the ZnTe nanobelts are a *p*-type material. According to previous studies of bulk ZnTe materials, these *p*-type characteristics could arise from the presence of Zn vacancies.<sup>[11]</sup> Figure 4d shows  $I_{\text{ds}}-V_{\text{ds}}$  curves at various temperatures with  $V_{\text{g}} = 0$  V. These curves are symmetric but not linear, which indicates a non-ohmic contact behavior between the electrodes and the ZnTe nanobelt.

In conclusion, we have succeeded in preparing high-quality ZnTe nanobelts with extremely narrow thickness (<6 nm) in a procedure using the high-boiling-point solvent oleylamine. We have further determined that the ZnTe

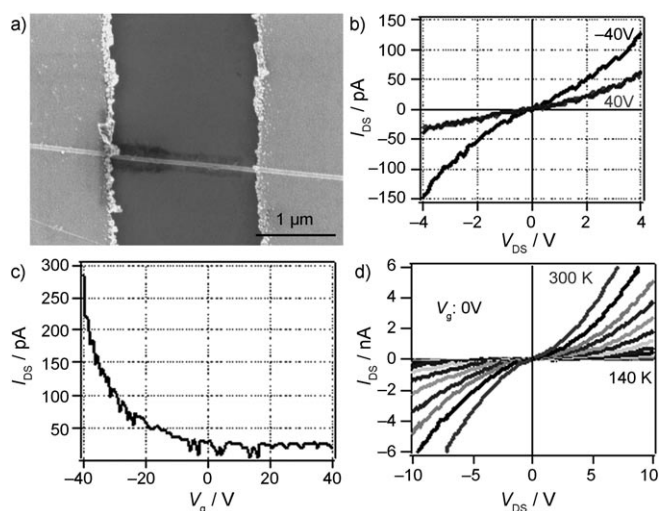


**Figure 4.** a) The SEM image of a single ZnTe nanobelt field-effect transistor (FET). The channel length is 2  $\mu\text{m}$ ; b) gate-dependent  $I_{\text{ds}}-V_{\text{ds}}$  curves of a ZnTe nanobelt FET under gate bias ranging from  $-40\text{ V}$  to  $+40\text{ V}$  in  $40\text{ V}$  steps; c)  $I_{\text{ds}}-V_{\text{g}}$  curves of the ZnTe nanobelt FET at  $V_{\text{ds}} = 5\text{ V}$ . The threshold gate voltage ( $V_{\text{th}}$ ) is  $-28\text{ V}$ ; d)  $I_{\text{ds}}-V_{\text{g}}$  curves of the single ZnTe nanobelt at temperatures ranging from  $140\text{ K}$  to  $300\text{ K}$  in  $10\text{ K}$  steps.

nanobelts are a *p*-type single-crystal material, and grow anisotropically along the  $\langle 200 \rangle$  direction, which is different from the  $[111]$ -direction growth reported previously. An abnormal intensity ratio between the 220 and 111 peaks implies a perfect orientation of the straight nanobelts when they were slowly deposited on a surface-polished substrate, whereas its absorption at approximately  $350\text{ nm}$  is direct optical evidence for a quantum confinement effect. Such extremely thin 1D ZnTe nanobelts are promising building blocks for the further development of nanodevices, such as field-effect nanotransistors.

### Experimental Section

In a typical experiment, oleylamine (15 mL, Aldrich, 70%) containing anhydrous zinc chloride (0.20 g, Aldrich, 99.995%) was heated to  $120^\circ\text{C}$  and stirred gently in a 100 mL three-neck flask. The system was subsequently placed under vacuum at  $120^\circ\text{C}$  for 20 min, and a clear solution formed. The temperature was then increased to  $250^\circ\text{C}$  and a pre-prepared solution of Te-TOP (1 mL, 1.0 M with respect to Te; trioctylphosphine (TOP), Aldrich, 90%, Te, Aldrich, 99.99%)<sup>[12]</sup> was injected into the gently stirred mixture under an argon stream. The system was kept at the same temperature for 10 min, and then cooled to room temperature after quickly removing the heating source. The products were isolated by addition of ethanol and were collected by centrifugation. The resulting ZnTe nanobelts can be redispersed in hexane (or toluene) and suspended for a short period of time after shaking.

The morphology and phase structure were evaluated using Hitachi 7600 & 9500 and HD 2000 transmission electron microscopes, Hitachi 4800 and Carl Zeiss Supra 55VP field-emission scanning electron microscopes, and a PANalytical X-pert system X-ray diffractometer with  $\text{CuK}\alpha_1$  radiation. UV/Vis spectra were recorded using a Cary 50 UV spectrophotometer from Varian Inc. Highly oriented XRD samples were prepared by following a procedure described elsewhere.<sup>[13]</sup> For the preparation of XRD samples, straight nanobelts were redispersed in toluene, this suspension was then transferred into a vial (without a cap) containing a piece of surface-polished (100) silicon wafer on the bottom. The nanobelts were slowly deposited onto the substrate; it was presumed that only the (220) facet should be aligned “face up” based on the “belt” morphology hypothesis. To evaluate the nanobelt transportation characteristics, a suspension of ZnTe nanobelts in hexane was deposited onto a degenerately doped Si wafer. Photolithography was then performed, followed by Ti/Au deposition to pattern the source and drain electrodes on both ends of the selected nanobelt by following a procedure described elsewhere.<sup>[14,15]</sup> All the electrical measurements were carried out using a semiconductor parameter analyzer (Agilent 4156B apparatus).

Received: August 18, 2008

Published online: October 29, 2008

**Keywords:** anisotropic growth · field-effect transistors · semiconductors · tellurium · zinc

- [1] T. Mahalingam, V. S. John, S. Rajendran, P. J. Sebastian, *Semicond. Sci. Technol.* **2002**, *17*, 465–470.
- [2] L. Li, Y. Yang, X. Huang, G. Li, L. Zhang, *J. Phys. Chem. B* **2005**, *109*, 12394–12398.
- [3] K.-T. Yong, Y. Sahoo, H. Zeng, M. T. Swihart, J. R. Minter, P. N. Prasad, *Chem. Mater.* **2007**, *19*, 4108–4110.
- [4] Z. W. Pan, Z. R. Dai, Z. L. Wang, *Science* **2001**, *291*, 1947–1949.
- [5] ICDD PDF card No. 15-0746.
- [6] Another possible morphology is tetragonal, that is, the “wire” has a more square cross-section. Based on the UV/Vis and SEM observations, this probability is very low.
- [7] Z. L. Wang, *J. Phys. Chem. B* **2000**, *104*, 1153–1175.
- [8] Y. Xiong, Y. Xia, *Adv. Mater.* **2007**, *19*, 3385–3391.
- [9] J. Zhang, K. Sun, A. Kumbhar, J. Fang, *J. Phys. Chem. C* **2008**, *112*, 5454–5458.
- [10] C. Wang, Y. Hou, J. Kim, S. Sun, *Angew. Chem.* **2007**, *119*, 6449–6451; *Angew. Chem. Int. Ed.* **2007**, *46*, 6333–6335.
- [11] H. B. Huo, L. Dai, C. Liu, L. P. You, W. Q. Yang, R. M. Ma, G. Z. Ran, G. G. Qin, *Nanotechnology* **2006**, *17*, 5912–5915.
- [12] Q. Liu, W. Lu, A. Ma, J. Tang, J. Lin, J. Fang, *J. Am. Chem. Soc.* **2005**, *127*, 5276–5277.
- [13] W. Lu, Q. Liu, Z. Sun, J. He, C. Ezeolu, J. Fang, *J. Am. Chem. Soc.* **2008**, *130*, 6983–6991.
- [14] Z. Liu, D. Zhang, S. Han, C. Li, T. Tang, W. Jin, X. Liu, B. Lei, C. Zhou, *Adv. Mater.* **2003**, *15*, 1754–1757.
- [15] C. Li, D. Zhang, S. Han, X. Liu, T. Tang, W. Jin, C. Zhou, *Adv. Mater.* **2003**, *15*, 143–145.